ATLANTIS PRESS

Advances in Intelligent Systems Research, volume 143

2nd International Conference on Applied Mathematics, Modelling and Statistics Application (AMMSA 2018)

Frequency Reduction-Based Model Predictive Direct Power Control with Multi-Cost Function

Qinghua Cui[1], Mian Liao[2], Zhiling Liao[1] and Zhaoling Chen[1]

[1]School of Electrical and Information Engineering, Jiangsu University, Zhenjiang, Jiangsu, China

[2]The Bradley Department of Electrical and Computer Engineer, Virginia Polytechnic Institute and State University, Blacksburg, Virginia, USA

***Abstract*—Model predictive direct power control (MPDPC) is one of the effective control strategies of the three phase inverter. However, a high sampling frequency is usually needed to realize the quick power tracking, which causes unnecessary switching loss. Frequency reduction-based MPDPC with single-cost function can limit the switching actions effectively. But it is difficult to choose a suitable coefficient. This paper proposes an improved frequency reduction-based MPDPC with multi-cost function, which can reduce the switching frequency and ensure the stability of power tracking at the same time. The proposed strategy was verified by simulation and experiment.**

Keywords—model predictive direct power control; switching function; multi-cost function; frequency reduction

I. INTRODUCTION

Recently, MPDPC was proposed to be applied in the control of the inverter [1], which combines the model predictive control (MPC) and direct power control (DPC). The MPDPC is similar to the DPC in that it selects one voltage vector for the next control period. However, their vector selection principles are fundamentally different. The complete model and future state of the inverter are taken into account in the MPDPC. A cost function containing power errors is defined to evaluate the effect of each voltage vector and the one minimizing the cost function is selected. The vector is selected by predicting the future state in the MPDPC, which will be more accurate and effective than the one chosen from the switching table of the DPC [2].

To maintain accurate power tracking of inverter, a higher sampling frequency is usually required in MPDPC. However, high sampling frequency results in a large number of switching loss. In order to avoid unnecessary switching actions and reduce the power loss, vector preselection technique is applied to MPDPC in [3]. This strategy reduces the switching loss, but its selection process is intricacy and the operation time is increased. The most commonly used method to reduce switching loss is lowering the switching frequency. But for the sake of realizing the stability of the system power tracking, the switching frequency should not be lowered too much. Frequency reduction algorithms for MPC is applied to electric motors in [4-5]. But the amount of their calculations is heavy, and the unnecessary switching actions are not completely eliminated. The cost function of MPDPC is flexible in form. It can contain multiple variables in one formula to implement multiple control targets [6]. The most common measure of reducing switching frequency is adding a switching item to the cost function, which is on behalf of switching frequency [7-8]. Switching frequency reduction was respectively introduced in [9] and [10] for current control of neutral point clamped (NPC) multilevel converters and three phase two level voltage source inverters. The transistor commutations can be reduced by predicting the number of switching. What we should care about is the steady state performance degradation caused by switching frequency reduction, which influences the normal operation of the system seriously. In order to realize accurate tracking of power, power compensation is introduced in [11]. This method stabilizes power fluctuations when the switching frequency is reduced. Large power fluctuations are also appeared in the process of dynamic transformation in the low frequency environment. Therefore, further studies on guaranteeing the stability of system running without increasing the complexity of the control strategy are needed when the switching frequency is reduced.

This paper proposes a frequency-reduction based MPDPC with multi-cost function strategy for three phase inverters. The mathematical model of three phase grid inverter is first established. Then the principle of MPDPC is introduced. The single-cost function and multi-cost function MPDPC are deeply analyzed.

II. INVERTER MODEL

The main circuit topology of three phase grid-connected inverter is shown in Fig. 1. Three insulated gate bipolar transistor (IGBT) half-bridge units are connected to grid via three inductors L and resistors R. e_a, e_b, e_c are the three phase grid voltage.

DC current was transformed into three phase AC current through the three phase inverter. The mathematical model of the inverter can be described in the stationary α-β coordinates as

$$\begin{cases} u_\alpha = L\dfrac{di_\alpha}{dt} + Ri_\alpha + e_\alpha \\ u_\beta = L\dfrac{di_\beta}{dt} + Ri_\beta + e_\beta \end{cases} \tag{1}$$

where u_α, u_β are the inverter output voltage vectors, i_α, i_β are the line current vectors, e_α, e_β are the grid voltage vectors. Active power and reactive power can be calculated by

$$p = \frac{3}{2}\left(e_\alpha i_\alpha + e_\beta i_\beta\right) \tag{2}$$

$$q = \frac{3}{2}\left(e_\beta i_\alpha - e_\alpha i_\beta\right) \tag{3}$$

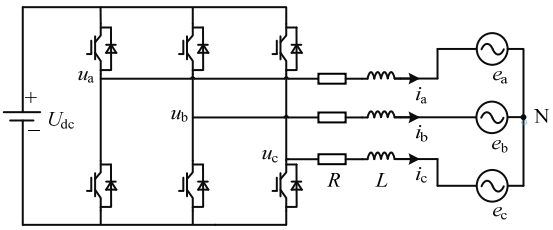

FIGURE I. DC/AC INVERTER STRUCTURE

III. MPDPC

Current discretization equation is got by forward difference, which uses linear first-order differential equations instead of current differential.

$$i_x^{k+1} = \left(1 - \frac{RT_s}{L}\right) i_x^k + \left(u_x^k - e_x^k\right)\frac{T_s}{L} \tag{4}$$

where x=α, β, i^{k+1} is the predictive grid-connected current at k+1th moment, i^k is the sampling current at kth moment and T_s is the time length of sampling period.

The sampling frequency is much higher than the frequency of the power grid voltage. As a result, the predictive value ek+1 can be approximately equal to the sampling value ek. The voltage vector rotates at the speed of ω rad/s, so ek+1 can also be expressed as

$$e_x^{k+1} = e_x^k e^{j\Delta\theta} \tag{5}$$

where $\Delta\theta$ is the offset angle of the voltage vector in one cycle.

The active and reactive power derivatives can be obtained from (3) and (4).

$$p^{k+1} = e_\alpha^{k+1} i_\alpha^{k+1} + e_\beta^{k+1} i_\beta^{k+1} \tag{6}$$

$$q^{k+1} = e_\beta^{k+1} i_\alpha^{k+1} - e_\alpha^{k+1} i_\beta^{k+1} \tag{7}$$

The block diagram of three phase grid inverter MPDPC strategy is shown in Fig. 2. Different voltage vectors cause their own active and reactive power changes. Therefore, there are many ways to choose the appropriate switch state to control the active and reactive power.

By evaluating the effect of each voltage vector on the active and reactive powers according to the cost function, the voltage vector that produces the least power ripple will be determined. In the inverter control, the control objective is chosen as the power factor of the ac output, which can be regulated by controlling the active power P* and reactive power Q*, respectively. Q* is usually set to 0 to achieve unity power factor operation.

$$F = \left|P^* - P^{k+1}\right| + \left|Q^* - Q^{k+1}\right| \tag{8}$$

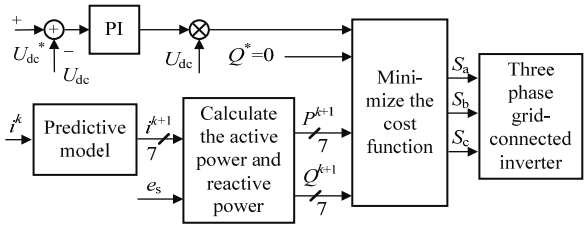

FIGURE II. MPDPC STRATEGY

IV. FREQUENCY REDUCTION-BASED MPDPC

When the three phase inverter switching frequency is high, the switching loss will also increase accordingly. The target of frequency reduction-based MPDPC is to reduce the frequency and lower the switching loss under premise of maintaining the stability of the three phase grid inverter. Fig. 3 shows the possible path of the switch movement at the next moment. Optimal state is on the premise of the minimum switching actions and system can still run stably.

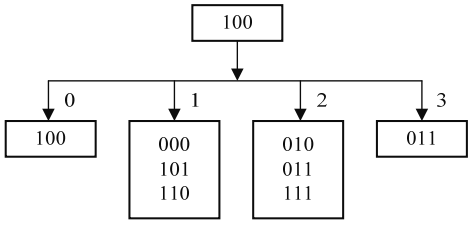

FIGURE III. SWITCHING ACTION PATHS

A. Single-Cost Function Frequency Reduction Strategy

In order to reduce the frequency of three phase grid inverter that works under MPDPC, the switching action is added to the cost function, as shown in

$$N = \sum_{i=a,b,c} \left|S_i^{k+1} - S_i^{k+1}\right| \tag{9}$$

where Sik and Sik+1 represent the current switching state and the predictive state in the next period separately. If S is 0, the upper transistor is off and the lower one is on, and 1 is the opposite. If the current vector is V0(000) and the next effective vector is V4(011), then Sak=0, Sbk=0, Sck=0, Sak+1=0, Sbk+1=1, Sck+1=1.

$$N = |0-0| + |1-0| + |1-0| = 2 \tag{10}$$

Therefore, frequency reduction-based MPDPC with constant coefficient can be expressed as

$$J = \left|P^* - P^{k+1}\right| + \left|Q^* - Q^{k+1}\right| + \lambda_1 \left(\sum_{i=a,b,c} \left|S_i^{k+1} - S_i^k\right| \right) \tag{11}$$

where P* is the rated active power, and Q* is the rated reactive power, Pk+1 and Qk+1 are the predictive active and reactive power separately. The first part of the formula is designed to track the active power and the reactive power and reduce the power ripple. The function of the second one is to reduce the switching frequency. λ1 is the magnification of the switching actions, which is a constant value.

V_0 and V_7 have the same effect to the change of power in the MPDPC. However, V_0 and V_7 represent different switch states, which have an important influence on the optimal vector choice. Two vectors should be considered separately in order to get the best switching actions. To sum up, frequency reduction-based MPDPC with constant coefficient can track the power and reduce the switching frequency at the same time.

B. Multi-Cost Function Frequency Reduction Strategy

From the foregoing analysis, we know that only one cost function is used in the frequency-reduction strategy. To facilitate later analysis, this frequency-reduction strategy is called single-function frequency-reduction model predictive direct power control. Although the single-function frequency-reduction control strategy can effectively reduce the switching frequency. However, λ_1 is a fixed value. If λ_1 is too small, the effect of frequency reduction cannot be achieved. If λ_1 is too large, when the inverter stably tracks a given power, λ_1 will occupy a dominant position in the cost function compared to a small power error, and the switching frequency will be greatly reduced, resulting in great current and power ripples. More serious, the stable operation of the system will be affected. Suppose that the vector working in the current cycle is U1 (100), and in the next cycle, the vector of the power tracking error from small to large is U4 (011), U6 (101), U1 (100). However, in the three vectors, the order of the number of switching operations from low to high is U1(100), U6(101), U4(011). When λ_1 dominates the cost function, the system will use U1 in the next cycle. From the above analysis, we can see that U1 is not an optimal choice. Using U1 will greatly reduce the switching actions, however, it also affects the stable tracking of power and is bound to cause a large amount of power ripples. Therefore, the coefficients of the switching function in the single-function frequency-reduction model predictive direct power control is not easy to select. The switching function is added to the cost function to reduce the switching frequency and reduce the loss. However, the main goal of the model predictive direct power control is still to achieve stable power tracking. It is only meaningful to reduce the switching frequency while ensuring the stable operation of the system.

The multi-cost function under the basis of existing frequency-reduction strategy is proposed to improve the contradiction between power tracking performance and low frequency loss. The multi-cost function is formally composed of multiple sets of cost functions including power error and switching function, as shown in equation (12). Where m1, m2, and m3 are the coefficients of the switching function, respectively, and their values are different.

$$\begin{cases} J = \left|P^* - Q^{k+1}\right| + \left|Q^* - Q^{k+1}\right| + \mathrm{m}_1 \left(\sum_{i=a,b,c} \left|\mathrm{S}_i^{k+1} - \mathrm{S}_i^k\right| \right) \\ J = \left|P^* - Q^{k+1}\right| + \left|Q^* - Q^{k+1}\right| + \mathrm{m}_2 \left(\sum_{i=a,b,c} \left|\mathrm{S}_i^{k+1} - \mathrm{S}_i^k\right| \right) \\ J = \left|P^* - Q^{k+1}\right| + \left|Q^* - Q^{k+1}\right| + \mathrm{m}_3 \left(\sum_{i=a,b,c} \left|\mathrm{S}_i^{k+1} - \mathrm{S}_i^k\right| \right) \end{cases} \tag{12}$$

Method one: power errors separate. The coefficients of the switching function are determined according to the system active power and reactive power error values.

If $|p^{k+1}-p_{\mathrm{ref}}|>p_{\max}$, n=n+1;

If $|q^{k+1}-q_{\mathrm{ref}}|>q_{\max}$, n=n+2.

Then the switching function coefficients m_1, m_2, m_3 are determined according to the judgment value n;

When n=0, it indicates that the active power error and reactive power error are within the allowable range.

When n=1, it indicates that the reactive power error is within the allowable range, and the active power error exceeds the limit. In this case, the value of the switching function coefficient should be properly reduced and the value m_2 should be used. At this time, m_2 should be smaller than m_1.

When n=2, it indicates that the active power error is within the allowable range, and the reactive power error exceeds the limit. The situation is similar to n=1, and its switching function coefficient also takes m_2.

When n=3, it indicates that the active power error and reactive power error exceed the maximum allowable range. In this case, power tracking should be the current priority. At this point, m_3=0. The switching function is removed from the cost function to ensure that the system can quickly resume stable operation.

Method two: power error merging. As shown in figure 4.20, the coefficients of the switching function are determined based on the sum of the absolute error value in active power and reactive power. In this strategy, the initial value of n is selected as 0.

If $|p^{k+1}-p_{\mathrm{ref}}|+|q^{k+1}-q_{\mathrm{ref}}|\leq W_1$, n=0;

If $W_1<|p^{k+1}-p_{\mathrm{ref}}|+|q^{k+1}-q_{\mathrm{ref}}|<W_2$, n=1;

If $|p^{k+1}-p_{\mathrm{ref}}|+|q^{k+1}-q_{\mathrm{ref}}|\geq W_2$, n=2;

In the equation above, W_1 and W_2 are the limits of the sum of the active and reactive power errors set according to the system operation, and $W_1<W_2$.

When n=0, the error value is the smallest at this moment, m_1 should take the maximum value.

When n=1, the error value is in the middle and the value of m_2 is properly reduced.

When n=2, the maximum error value at this moment, m_3 is taken as 0.

Through the above analysis, we can see that if you can take more cost function group, then the performance of the system will achieve a more complete effect.

Taking $W_1<W_2<W_3<W_4<W_5<...$, when $|p^{k+1}-p_{ref}|+|q^{k+1}-q_{ref}|$ gradually increases, the value of m also gradually decreases. The size of m in different systems should not be the same. The specific value depends on the system.

From the above analysis, we can see that the more error limit values are used, the smoother the change of m value is. But too many values are not conducive to system design and mutation. Assuming a sudden power change, the power error will also change. But the error limits have not changed, which may cause the system performance to decline. Therefore, it is relatively appropriate to set the error limits to 5 or so. When the system mutates, it is also more convenient to change the system error limits.

TABLE I. PARAMETERS OF MAIN CIRCUIT

DC voltage	u_{DC}	200V
Line equivalent resistance	R	0.2Ω
Filter inductance	L	10mH
Phase voltage amplitude	e_{max}	70.7V
Phase voltage frequency	f	50Hz
Time step	T_s	5E-005s

V. SIMULATION AND EXPERIMENTAL RESULTS

A. Simulation Results

In order to verify the validity of the proposed control strategy, the MPDPC, the single cost function MPDPC and the multi-cost function MPDPC are simulated in the PSIM environment. The parameters of the system are shown in TABLE I. For the sake of convenience, the above three control strategies are defined as MPDPC.I, MPDPC.II and MPDPC.III. The rated active power and reactive power are set 1000w and 0Var to ensure the system running under unit power factor.

TABLE II. COMPARISON OF SIMULATION RESULTS

Control Strategy	Average switching frequency	Current THD
MPDPC.I	9489	4.461
MPDPC.II	5800	6.066
MPDPC.III	5714	4.690

TABLE II shows the average switching frequency and current THD of MPDPC.I, MPDPC.II and MPDPC.III. Since the switching frequency of MPDPC is not constant, the average switching frequency is obtained by counting the total number of switching operations divided by 6 in one second. From the TABLE II, the switching frequency of MPDPC.II is reduced significantly compared with MPDPC.I.

But it also has a greatly bad impact on the current THD, which is not conducive to the system steady operation. MPDPC.III highlights a great advantage. The switching frequency of MPDPC.III has a substantial reduction. What's more, it still maintains a high level of output current waveform.

Fig.4, Fig.5 and Fig.6 are the a-phase current waveform of MPDPC.I, MPDPC.II and MPDPC.III respectively. The comparison shows that MPDPC.II current waveform produces large distortion, which has a bad effect on the stable operation of the system. MPDPC.III achieves the optimal selection of the vector, which still outputs a good current waveform even in the case of switching frequency reduction.

Fig. 7, Fig. 8 and Fig. 9 are the active and reactive power waveforms of MPDPC.I, MPDPC.II and MPDPC.III respectively. Active and reactive power of MPDPC.II have a large number of spikes. However, MPDPC.III causes relatively little interferences.

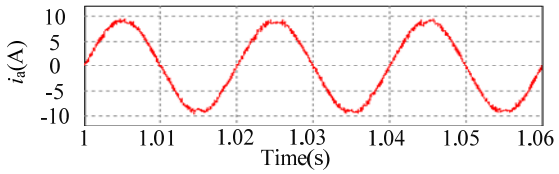

FIGURE IV. MPDPC.I CURRENT WAVEFORM

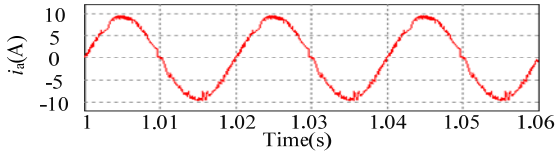

FIGURE V. MPDPC.II CURRENT WAVEFORM

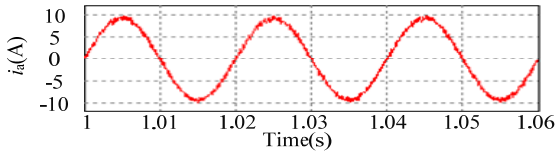

FIGURE VI. MPDPC.III CURRENT WAVEFORM

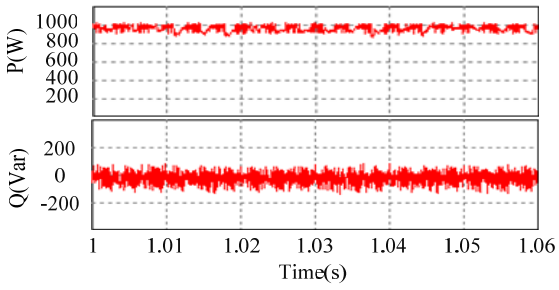

FIGURE VII. ACTIVE AND REACTIVE POWER WAVEFORMS IN MPDPC.I

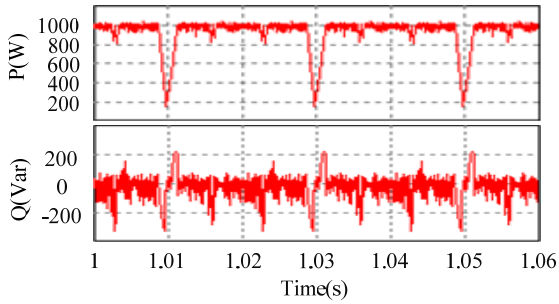

FIGURE VIII. ACTIVE AND REACTIVE POWER WAVEFORMS IN MPDPC.II

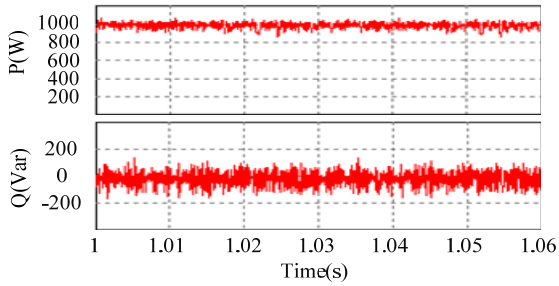

FIGURE IX. ACTIVE AND REACTIVE POWER WAVEFORMS IN MPDPC.III

B. Experimental Tests

Fig.10, Fig.11 and Fig.12 are the experimental waveforms of MPDPC.I, MPDPC.II and MPDPC.III respectively. Comparing MPDPC.II and MPDPC.III, it can be found that the burr peak in MPDPC.III is reduced much, which proves that MPDPC.III can effectively achieve the performance improvement of frequency-reduction strategy.

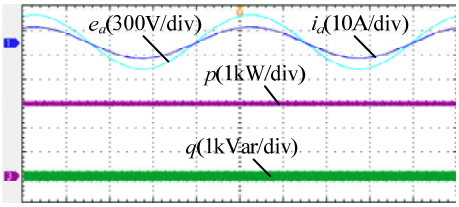

FIGURE X. EXPERIMENT WAVEFORMS OF MPDPC.I

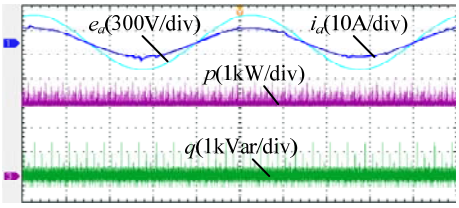

FIGURE XI. EXPERIMENT WAVEFORMS OF MPDPC.II

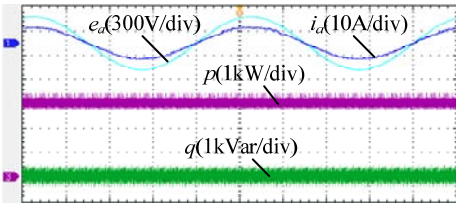

FIGURE XII. EXPERIMENT WAVEFORMS OF MPDPC.III

VI. CONCLUSIONS

This paper proposes a low frequency MPDPC with multi-cost function strategy for three phase inverters. This strategy optimizes the selection of vector. The multi-cost function MPDPC can ensure the frequency reduction, which lower the switching loss, and maintain the high-quality system operation at the same time. The coefficient in the single-cost function MPDPC cannot be determined easily and cannot adapt according to the system power changes. The cost function in this paper is redefined. Using the proposed strategy, the defect of the constant coefficient MPDPC is solved. Based on the comparison of simulation, the validity of the frequency reduction-based MPDPC with variable coefficient is verified.

REFERENCES

[1] Patricio Cortes, Jose Rodriguez, Patrycjusz Antoniewicz and Marian Kazmierkowski, “Direct power control of an AFE using predictive control”, Power Electronics, IEEE Transactions on, vol. 23, no. 5, pp. 2516-2523, 2008.

[2] Yongchang Zhang, Wei Xie, Zhengxi Li and Yingchao Zhang, “Model predictive direct power control of a PWM rectifier with duty cycle optimization,” Power Electronics, IEEE Transactions on, vol. 28, no. 11, pp. 5343-5351, 2013.

[3] Sangshin Kwak, Jun-Cheol Park, “Model-Predictive Direct Power Control With Vector Preselection Technique for Highly Efficient Active Rectifiers,” Industrial Informatics, IEEE Transactions on, vol. 11, no. 1, pp. 44-52, 2015.

[4] Matthias Preindl, Erik Schaltz and Paul Thogersen, “Switching frequency reduction using model predictive direct current control for high-power voltage source inverters,” Industrial Electronics, IEEE Transactions on, vol. 58, no. 7, pp. 2826-2835, 2011.

[5] Tobias Geyer, Georgios Papafotiou and Manfred Morari, “Model predictive direct torque control–part I: Concept, algorithm, and analysis,” vol. 56, no. 6, pp. 1894-1905, 2009.

[6] Xiao Li, Mohammad B. Shadmand, Robert S. Balog, Haitham Abu Rub, “A Harmonic Constrained Minimum Energy Controller for a Single-phase Grid-tied Inverter Using Model Predictive Control,” 2015 IEEE Energy Conversion Congress & Exposition, pp. 5153-5159, 2015.

[7] Rene Vargas, Jose Rodriguez, Christian A. Rojas and Marco Rivera, “Predictive control of an induction machine fed by a matrix converter with increased efficiency and reduced common-mode voltage,” Energy Conversion, IEEE Transactions on, vol. 29, no. 2, pp. 473-485, 2014.

[8] Jose Rodriguez, Marian P. kazmierkowski, Jose R. Espinoza, et al. “State of the art of finite control set model predictive control in power electronics,” Industrial Informatics, IEEE Transactions on, vol. 9, no. 2, pp. 1003-1016, 2013.

[9] Rene Vargas, Patricio Cortes, Ulrich Ammann, Jose Rodriguez and Jorge Pontt, “Predictive control of a three-phase neutral-point-clamped inverter,” Industrial Electronics, IEEE Transactions on, vol. 54, no. 5, pp. 2697-2705, 2007.

[10] Matthias Preindl, Erik Schaltz and Paul Thogersen, “Switching frequency reduction using model predictive direct current control for high-power voltage sources inverters,” Industrial Electronics, IEEE Transactions on, vol. 58, no. 7, pp. 2826-2835, 2011.

[11] Jiefeng Hu, Jianguo Zhu, Gang Lei, Glenn Platt, “Multi-Objective Model-Predictive Control for High-Power Converters,” Energy Conversion, IEEE Transactions on, vol. 28, no. 3, pp. 652-663, 2013.